ISSN: 0067-2904

Effect of Inclined MHD Peristaltic Transport for non-Newtonian model in a Non-Uniform Channel Through Porous Medium As: HTF

Safa Riyadh Ridha[1], Hussam Numan Solagh[2]*

[1]*Registration and Student Affairs, Head of University, Ibn Sina University for Medical Sciences, Baghdad, Iraq*
[2]*Scientific Affairs, Head of University, Mustansiriyah University, Baghdad, Iraq*

Received: 29/10/2023 Accepted: 27/1/2024 Published: xx

Abstract

The current work aims to study the effect of an inclined magnetohydro dynamics peristaltic transport of a non-Newtonian hyperbolic tangent fluid in a non-uniform channel via porous medium. The nonlinear governing equations regarding hyperbolic tangent fluid have been studied and solved analytically with the use of a regular perturbation approach under considerations of a long wavelength as well as low Reynolds number. All computational results are also discussed graphically using the MATHEMATICA program. The mathematical expressions for axial velocity and stream functions have been derived analytically. Different physical parameters have been shown graphically and discussed it's effect. It is established that increasing the Hartmann number and the parameter of porosity will increase the velocity and the quantity of boluses. While the size of boluses decreases by increasing the magnetic field inclination angle. Moreover, Some mathematical and engineering aspects of non-Newtonian fluids are investigated in the current analysis.

Keywords: Inclined MHD Peristaltic Motion; Hyperbolic Tangent Fluid (HTF); Non-Uniform channel; Porous Medium. Perturbation Method.

تأثير الهيدروديناميكية المغناطيسية المائلة على الحركة التمعجية لنموذج غير نيوتوني في قناة غير مسامي: مائع الظل الزائدي منتظمة خلال وسط

صفا رياض رضا[1], حسام نعمان صولاغ*[2]

[1]التسجيل وشؤون الطلبة، رئاسة الجامعة، جامعة ابن سينا للعلوم الطبية، بغداد، العراق

[2]الشؤون العلمية، رئاسة الجامعة، الجامعة المستنصرية، بغداد، العراق

الخلاصة

هذا العمل يهدف الى دراسة تأثير الهيدروديناميكا المغناطيسية المائلة على الحركة التمعجية لنموذج غير نيوتوني (مائع الظل الزائدي) في قناة غير منتظمة عبر وسط مسامي. تم دراسة وحل المعادلات الحاكمة غير الخطية المتعلقة بمائع الظل الزائدي تحليلياً باستخدام طريقة الاضطراب المنتظم تحت فرضيات الطول الموجي الطويل بالإضافة إلى رقم رينولدز المنخفض و تمت مناقشة جميع النتائج الحسابية بيانيا بأستخدام برنامج "MATHEMATICA". تم اشتقاق الصيغ الرياضية للسرعة المحورية و دالة التدفق. تم عرض المعلمات الفيزيائية المختلفة بيانيا و مناقشة تأثيرها. لقد ثبت أنه بزيادة عدد هارتمان ومعلمة المسامية تزداد السرعة وكمية

*Email: Hussam.n.solagh@uomustansiriyah.edu.iq

و حجم البلعات بينما يتناقص حجم البلعات بزيادة زاوية ميل المجال المغناطيسي.علاوة على ذلك، تم استكشاف الجوانب الهندسية والرياضية للسوائل غير النيوتونية في التحليل الحالي.

Nomenclature

(x,y) **:** The cartesian coordinates in a wave frame.
$(\bar{X}, \bar{Y})$: The cartesian coordinates in a fixed frame.
$(\bar{U}, \bar{V})$:The velocity components of the fixed frame.
(u, v) :The velocity components of the wave frame.
p : The pressure in the wave of reference.
$\bar{P}$: The pressure in the fixed frame of reference.
$\bar{a}_1, \bar{a}_2$: The amplitudes of the waves at the lower and upper wall of channel, respectively.
$\bar{d}_1, \bar{d}_2$: The widths of the channel.
λ : The wavelength.
Φ : The phase difference.
C The wave speed.
t : Time.
$\bar{\tau}$: The extra stress tensor.
Γ : The time dependent constant.
μ_0 : The 0-shear rate viscosity.
μ_∞ :The infinite shear rate viscosity.
n : The power – law index.
$\dot{\gamma}$: The shear rate.
ρ : The density fluid.
μ_0 : The dynamic viscosity.
β_0 : The constant magnetic field.
$\dot{\beta}$: The magnetic field inclination angle.
σ : The electrical conductivity.
K : The porosity of porous media.
$\bar{S}_{\bar{X}\bar{X}}, \bar{S}_{\bar{X}\bar{Y}}, \bar{S}_{\bar{Y}\bar{Y}}$: The extra stress tensor components, respectively.
Π :The second invariant strain tensor.
δ : The wave number.
Re :The Reynolds number.
M : The Hartmann number.
We : The Weissenberg number.
F : The dimensionless time average flow rate in a wave frame.
$\bar{Q}$: The time average flux in a fixed frame.
Q : The time average flow rate.
ψ : The stream function.

1. Introduction

Peristalsis is the scientific term for the movement of fluid along of a channel's axis as a result of the relaxation and contraction of its walls. Due to its intriguing possibilities, peristaltic flow has attracted attention of numerous engineers and scientists. Non-Newtonian and Newtonian flows are discussed. Nowadays, scientific and technological research are being done on the peristaltic phenomenon. The word peristalsis is originated from Greek word peristaltkos which means the compressing and clasping. The non-Newtonian fluid peristaltic flow could be defined as a new field that is presently being studied. The bio-medical and engineering fields have several applications for such phenomena that are quite significant. This is due to the fact that it has numerous practical uses, including those in biomedical engineering,

geophysics, cancer treatment, and blood pumping devices. The first study was conducted in 1964 by Latham [1], who worked on a peristaltic pump and showed how peristaltic flow works in a channel. The peristalsis phenomena were next explored by Shapiro et al. [2] in a channel which is geometrically 2D. Although, they used the low lubrication theory assumptions that obscure numerous inertial effects which must be discussed. In addition, they provided theoretical findings for the two planes. With regard to an infinite channel, peristalsis was studied by Yih and Fung [3]. Theoretical research on peristaltic motion in non-Newtonian and Newtonian fluids is considerable. The non-Newtonian qualities can be found in physiological liquids like blood and food bolus fluid, geological suspensions like sedimentary liquids and drilling muds, as well as industrial liquids like oil and grease and biotechnological liquids like polymers, gels, and food products.

One of the most significant liquid models in a non-Newtonian liquid category, which is vital in peristaltic system, is the model of hyperbolic tangent fluid flow due to its applications in filtration, aquifer transport advancements, chemical industry separation processes, groundwater pollution, and transpiration cooling. The non-Newtonian fluid flow study through porous media has attracted a great deal of attention. In this work, the hyperbolic tangent fluid model is used to examine the non-Newtonian fluids' flow characteristics.

In the majority of experiments, Ingham and Pop's [4] and Akram and Nadeem's [5] studied the peristaltic transport which is related to the Hyperbolic Tangent fluids within asymmetric channel that is originally utilized this model. With the aid of the Homotopic perturbation approach, Maraj and Nadeem [6] investigated mathematically the peristaltic motion regarding to the hyperbolic tangent fluid in curved channel. Nadvinamani *et al.* [7] discussed the dynamics of a hyperbolic tangent fluid passing through tapered asymmetrical porous channel. A different study is found that the MHD effect on peristaltic transport is significant in a broad range of the fields, which includes technology (MHD pump) and biology (blood flow). Through the use of a porous medium, Hayat *et al*. [8] studied the effect of the Dufour and Soret on MHD peristaltic mechanism of the Jeffery fluid. Nadem and Akram [9] studied and investigated the peristaltic flow of the MHD hyperbolic tangent fluid in the vertical asymmetrical channel with heat transfer. Through considering mass and heat transfer, Saravana *etal*. [10] have theoretically studied the MHD peristaltic flow of the hyperbolic tangent fluid in the non-uniform channels. Other studies on magnetohydrodynamic peristaltic flows can be found in [11], [12], [13], [14], [15], [16],[17],[18] and [19] as well as the references therein. Researches consulted on the peristaltic flow under magnetic field impacts in various circumstances. Akbar *et al*. [20] discussed the effects of the magnetic field on peristaltic transportation which is related to the Casson. Rashid *et al*. [21] have investigated impacts of the induced magnetic field on Williamson fluid's peristaltic flow along curved channel. The magnetic fluid was shown by Sucharitha *et al.* [22] inside inclined, non-uniform, porous channel that has flexible walls. With regard to a tapered asymmetric channel, Prakash and Kothadapani [23] investigated the peristaltic flow of Carreau nano-fluid under impact of magnetic fields. Regarding to the peristaltic pumping of the hyperbolic tangent nano-fluid in non-uniform channel and induced magnetic field, Akram *et al.* [24] studied thermal and concentration convection. Yellamma *et al*. [25] studied the triple diffusive Marangoni convection Marangoni-convection (TDMC) problem when a steady heat source is present in both layers and a vertical uniform magnetic field. In addition, . Balaji *et al*. [26] conducted an analytical work to study the effect of the thermal gradient and heat sources on the onset of convection using the Darcy model . They are also taken into account the study of the effects of local thermal non equilibrium(LTEN). Manjunatha and Sumithra [27] studied the problem of a non- Darcy double diffusive magneto Marangoni convection in a horizontally infinite two

layer. In another work, Sumithra and Manjunatha [28] investigated the problem of Bènard-Magneto-Marangoni convection in a composite layer in the presence of heat source in both layers.

Numerous peristaltic investigations have been done to look into the impact of magnetic fields for different fluid model configurations [29–32]. Recently, Ridha [33] presented a review study on the concepts, perspectives, and mathematical models of a non-Newtonian fluids including Hyperbolic tangent fluid. This study is concentrated on the peristaltic flow of non-Newtonian fluids. Discussion of the impact of inclined MHD peristaltic transport regarding hyperbolic tangent fluid in a non-uniform porous channel is the main goal of this work. The long wavelength and low Reynolds number assumptions are utilized in order to simplify the nonlinear partial differential equations related to a hyperbolic tangent fluid, and the resulting equations are numerically and analytically solved. The velocity and stream are analyzed and explained with the use of the Mathematica software. Finally, utilizing graphs of streamlines and the phenomena of trapping are also explored along with the behavior of other related physical parameters.

2. Mathematical Formulation of The Problem

We take into account the MHD peristaltic transport related to the non-Newtonian hyperbolic tangent fluid inside non-uniform porous channel. It is influenced by an inclination magnetic field $\boldsymbol{\beta}$ which acts along y-axis. Induced magnetic field has been disregarded for low magnetic Reynolds numbers. A sinusoidal wave train propagating through channel's flexible walls at constant wave speed, c, has been thought to have caused the medium. The problem's geometry model is shown in Figure 1. The following describes how peristaltic waves' flexible wall surface takes shape:

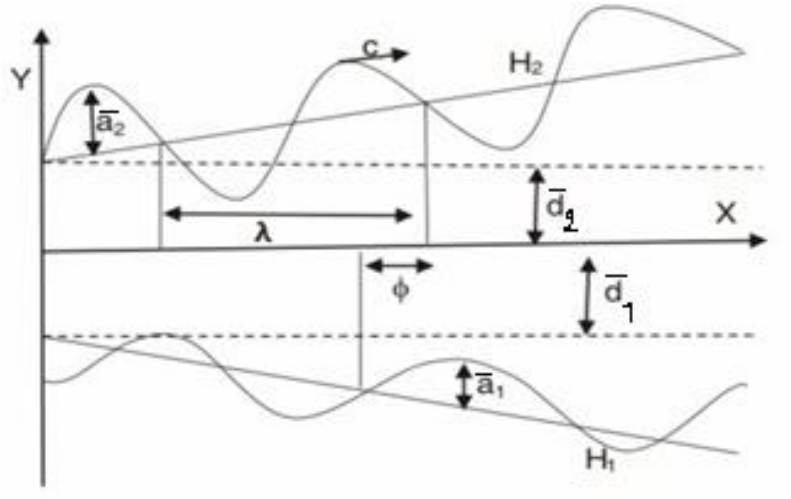

Figure1: Geometry Model of The Problem

The peristaltic waves geometry on flexible walls can be defined by the relation as follows:

$$Y= H_1 (\bar{X},t) = \bar{d}_1 + \bar{a}_1 \sin[\frac{2\pi}{\lambda}(\bar{X} - c\bar{t})] \ , \quad (1)$$

$$Y= H_2 (\bar{X},t) = - \bar{d}_2 - \bar{a}_2 \sin[\frac{2\pi}{\lambda}(\bar{X} - c\bar{t}) + \Phi]. \quad (2)$$

Equations (1) and (2) are the upper wall and lower wall, respectively. X - axis lies in wave propagation direction and Y - axis is to be perpendicular to the value of X . It has been noted that $\Phi= 0$ is corresponding to a non-uniform channel with the waves out of phase and for $\Phi= \pi$ waves are in phase. Additionally, $\bar{a}_1$, $\bar{a}_2$, $\bar{d}_1$, $\bar{d}_2$ and Φ satisfy the following equation:

$$\bar{a}_1{}^2 + \bar{a}_2{}^2 + 2\,\bar{a}_1\,\bar{a}_2\cos(\Phi) \le (\bar{d}_1 + \bar{d}_2)^2 \,. \tag{3}$$

The Cauchy stress tensor in Tangent Hyperbolic non-Newtonian fluid can be expressed in the following form:

$$\bar{\tau} = -\,[\,\tilde{S}\tanh(\Gamma\dot{\gamma})^{n}]\dot{\gamma}\ , \tag{4}$$

$$\tilde{S} = \mu_\infty + (\mu_0 + \mu_\infty)\ , \tag{5}$$

$$\dot{\gamma} = \sqrt{\frac{1}{2}\sum_i\sum_j \gamma_{ij}\gamma_{ij}} = \sqrt{\frac{1}{2}\Pi}\ \ . \tag{6}$$

Under consideration of $\boldsymbol{\mu_\infty = 0}$, there is a possibility to discuss the problem for the infinite shear rate viscosity, thus, by consideration of tangent hyperbolic fluid describing effects that is $\boldsymbol{\Gamma\dot{\gamma}} \ll 1$. Then Eq.(4) $\bar{\tau}$ can be expressed as follows:

$$\begin{aligned}\bar{\tau} &= -\,\mu_0\,[(\Gamma\dot{\gamma})^n]\,\dot{\gamma} = -\,\mu_0\,[(1+\Gamma\dot{\gamma}-1)^n)]\dot{\gamma}\\ &= -\,\mu_0\,[1+n\,(\Gamma\dot{\gamma}-1)\,]\dot{\gamma}\ .\end{aligned} \tag{7}$$

3. The Governing Equations Formulation

The equations for fluid motion in a lab frame (X, Y) under impacts of an inclined magnetic field can be provided by:

$$\frac{\partial\bar{\mathrm{U}}}{\partial\bar{\mathrm{X}}} + \frac{\partial\bar{\mathrm{V}}}{\partial\bar{\mathrm{Y}}} = 0\ . \tag{8}$$

$$\rho\Big(\frac{\partial\bar{U}}{\partial\bar{\mathrm{t}}} + \bar{U}\frac{\partial\bar{U}}{\partial\bar{\mathrm{X}}} + \bar{\mathrm{V}}\frac{\partial\bar{\mathrm{U}}}{\partial\bar{\mathrm{Y}}}\Big) = -\frac{\partial\bar{\mathrm{P}}}{\partial\bar{\mathrm{X}}} + \frac{\partial\bar{S}_{\bar{X}\bar{X}}}{\partial\bar{\mathrm{X}}} + \frac{\partial\bar{S}_{\bar{X}\bar{Y}}}{\partial\bar{\mathrm{Y}}} - \sigma\,\beta_0^2\cos\dot{\beta}(\bar{\mathrm{U}}\cos\dot{\beta} - \bar{\mathrm{V}}\cos\dot{\beta}) - \frac{\mu_0}{k}\bar{\mathrm{U}} \tag{9}$$

.

$$\rho\Big(\frac{\partial\bar{V}}{\partial\bar{\mathrm{t}}} + \bar{U}\frac{\partial\bar{\mathrm{V}}}{\partial\bar{\mathrm{X}}} + \bar{\mathrm{V}}\frac{\partial\bar{\mathrm{V}}}{\partial\bar{\mathrm{Y}}}\Big) = -\frac{\partial\bar{\mathrm{P}}}{\partial\bar{\mathrm{Y}}} + \frac{\partial\bar{S}_{\bar{X}\bar{Y}}}{\partial\bar{\mathrm{X}}} + \frac{\partial\bar{S}_{\bar{Y}\bar{Y}}}{\partial\bar{\mathrm{Y}}} + \sigma\,\beta_0^2\sin\dot{\beta}\left(\bar{\mathrm{U}}\cos\dot{\beta} - \bar{\mathrm{V}}\sin\dot{\beta}\right) - \frac{\mu_0}{k}\bar{\mathrm{V}}. \tag{10}$$

Let us define a wave frame (x,y) that moves with velocity c away from fixed frame ($\bar{X}$, $\bar{Y}$) by the following expressions
$x=\bar{X}$-c$\bar{t}$, $y=\bar{Y}$, $u=\bar{U}$-c, $v=\bar{V}$ and $p\ (x,\ y)=\bar{P}\ (\bar{X},\ \bar{Y},\ \bar{t})$.

Defining the non - dimensional quantities as follows:

$$x = \frac{\partial\bar{X}}{\lambda},\ y = \frac{\partial\bar{Y}}{d},\ u = \frac{\partial\bar{U}}{c},\ v = \frac{\partial\bar{V}}{c},\ h_1 = \frac{\bar{h}_1}{\bar{d}_1},\ h_2 = \frac{\bar{h}_2}{\bar{d}_2},\ h = \frac{\bar{h}}{\bar{d}},\ \dot{\gamma} = \frac{\bar{\gamma}\,d}{c},\ p = \frac{\bar{d}^2}{c\lambda\mu_0}\bar{P}\ ,\ S_{xx} = \frac{d\bar{S}_{\bar{X}\bar{X}}}{c\mu_0}$$

$$S_{xy} = \frac{\lambda\bar{S}_{\bar{X}\bar{Y}}}{c\mu_0}\ ,\ S_{yy} = \frac{d\bar{S}_{\bar{Y}\bar{Y}}}{c\mu_0}\ ,\ t = \frac{c\,\bar{t}}{\lambda},\ Re = \frac{\rho\bar{d}C}{\mu_0},\ \delta = \frac{\bar{d}}{\lambda},\ M = \sqrt{\frac{\sigma}{\mu_0}}\,d\,\beta_0, We = \frac{\Gamma c}{\bar{d}},\ \sigma = \frac{\bar{d}}{\sqrt{K}},$$

$$\mathrm{Da} = \frac{k}{\bar{d}^2}, \beta_0 = \frac{\overline{\beta_0}}{\bar{d}},\ \theta = \frac{(\bar{T}-\overline{\mathrm{T}_0})}{(\bar{T}_1-\overline{\mathrm{T}_0})} \tag{11}$$

Then from Eqs. (9) and (10), it takes the form

$$Re\delta\left(\frac{\partial\mathrm{u}}{\partial\mathrm{t}} + \mathrm{u}\frac{\partial\mathrm{u}}{\partial\mathrm{x}} + \mathrm{v}\frac{\partial\mathrm{u}}{\partial\mathrm{y}}\right) = -\frac{\partial\mathrm{p}}{\partial\mathrm{x}} + \delta^2\frac{\partial S_{xx}}{\partial\mathrm{x}} + \frac{\partial S_{xy}}{\partial\mathrm{y}} - M^2\beta_0^2\cos\dot{\beta}\left(u\cos\dot{\beta} - \mathrm{v}\sin\dot{\beta}\right) + \frac{1}{Da}\mathrm{u}. \tag{12}$$

$$Re\delta^3\left(\frac{\partial\mathrm{u}}{\partial\mathrm{t}} + \mathrm{u}\frac{\partial\mathrm{v}}{\partial\mathrm{x}} + \mathrm{v}\frac{\partial\mathrm{v}}{\partial\mathrm{y}}\right) = -\frac{\partial\mathrm{p}}{\partial\bar{\mathrm{Y}}} + \delta^2\frac{\partial S_{xy}}{\partial\bar{\mathrm{X}}} + \delta\frac{\partial S_{yy}}{\partial\bar{\mathrm{Y}}} + M^2\beta_0^2\sin\dot{\beta}(u\cos\dot{\beta} - \mathrm{v}\sin\dot{\beta}) + \delta^2\frac{1}{Da} \tag{13}$$

Where

$$s_{xx} = -2[1+\mathrm{n}(We\,\dot{\gamma}-1)]\frac{\partial u}{\partial x},$$

$$s_{xy} = -[1+\mathrm{n}(We\,\dot{\gamma}-1)]\left(\frac{\partial u}{\partial y} - \delta^2\frac{\partial v}{\partial x}\right),$$

$$s_{yy} = 2\,\delta\,[1+\mathrm{n}(We\,\dot{\gamma}-1)]\frac{\partial\mathrm{v}}{\partial\mathrm{y}},$$

$$\dot{\gamma} = \left[2\,\delta^2\left(\frac{\partial v}{\partial x}\right)^2 + \left(\frac{\partial u}{\partial y} - \delta^2\frac{\partial v}{\partial x}\right)^2 + 2\delta^2\left(\frac{\partial v}{\partial x}\right)^2\right]^{\frac{1}{2}}.$$

Assuming that ψ is a stream function, then we have:

$\mathrm{v} = -\delta\frac{\partial \psi}{\partial \mathrm{x}}$, $\mathrm{u} = \frac{\partial \psi}{\partial \mathrm{y}}$.

The non-dimensional variables have been defined in Eqs.(14) and (15) which give the following equation.

$$Re\,\delta\left[\psi_y\frac{\partial}{\partial \mathrm{t}} + \psi_y\frac{\partial}{\partial \mathrm{x}} - \psi_x\frac{\partial}{\partial \mathrm{y}}\right]\psi_y = -\frac{\partial \mathrm{p}}{\partial \mathrm{x}} + \delta^2\frac{\partial S_{xx}}{\partial \mathrm{x}} + \frac{\partial S_{xy}}{\partial \mathrm{y}} - Ha^2\,\beta_0^2\cos\dot{\beta}\left(\psi_y\cos\dot{\beta} - \psi_x\sin\dot{\beta}\right) + \frac{1}{Da}\psi_y. \quad (14)$$

$$Re\,\delta^3\left[\psi_x\frac{\partial}{\partial \mathrm{t}} + \psi_y\frac{\partial}{\partial \mathrm{x}} - \psi_x\frac{\partial}{\partial \mathrm{y}}\right]\psi_x = -\frac{\partial \mathrm{p}}{\partial \mathrm{y}} + \delta^2\frac{\partial S_{xy}}{\partial \mathrm{x}} + \delta\frac{\partial S_{yy}}{\partial \mathrm{y}} + Ha^2\,\beta_0^2\sin\dot{\beta}\left(\psi_y\cos\dot{\beta} - \psi_x\sin\dot{\beta}\right) - \delta^2\frac{1}{Da}\psi_x. \quad (15)$$

Under assumptions of the long wave-length and small Reynolds number. approximations, we obtain the following expressions:

$$\frac{\partial \mathrm{p}}{\partial \mathrm{x}} = \frac{\partial s_{xy}}{\partial \mathrm{y}} - \left(M^2\cos^2\dot{\beta} - \frac{1}{K} + \sigma^2\right). \quad (16)$$

$$\frac{\partial \mathrm{p}}{\partial \mathrm{y}} = 0\,. \quad (17)$$

Where $s_{xy} = (1\text{-}n)\frac{\partial^2\psi}{\partial \mathrm{y}^2} + n\,We\left(\frac{\partial^2\psi}{\partial \mathrm{y}^2}\right)^2$.

The relevant boundary conditions in the terms of stream function can be represented in the following forms

$$\psi = \frac{\mathrm{F}}{2}, \frac{\partial \psi}{\partial \mathrm{y}} = -1 \quad \text{at } \mathrm{y} = h_1(\mathrm{x}) \quad (18)$$

$$\psi = -\frac{\mathrm{F}}{2}, \frac{\partial \psi}{\partial \mathrm{y}} = -1 \text{ at } \mathrm{y} = h_2(\mathrm{x}) \quad (19)$$

The flux at any of the axial stations in fixed frame can be expressed as follows:

$$\overline{\mathrm{Q}} = \int_{h2}^{h1}(u+1)dy = h1\text{-}\,h2\,+F\ . \quad (20\ \mathrm{a})$$

It is associated with dimensionless time average flow rate Q in lab frame based on:

$$Q = \frac{1}{T}\int_0^T \overline{\mathrm{Q}}\,dt\ = \frac{1}{T}\int_0^T (h1 - h2\ + F)\,dt = F+1+d\ . \quad (20\ \mathrm{b})$$

where $\mathrm{F} = \int_{h2(\mathrm{x})}^{h1(\mathrm{x})}\frac{\partial \psi}{\partial \mathrm{y}}dy = \psi(h_1(\mathrm{x})) - \psi\left(h_2(\mathrm{x})\right)$, (21)

$h_1(\mathrm{x})$ *and* $h_2(\mathrm{x})$ are dimensionless forms that can be represented by:

$$h_1(x) = 1+mx+a\,sin\,(2\pi\,(x\text{-}t)), \quad (22)$$

$$h_2(x) = -1\text{-}mx\text{-}b\,sin\,(2\pi\,(x\text{-}t)+\Phi),$$

where a,b, Φ & d satisfy the equation

$$a^2 + b^2 + 2ab\,cos(\Phi) \le (1+d)^2\,. \quad (23)$$

Eq. (17) indicates that $p \neq p(\mathrm{y})$, by the elimination of p from Eq. (16) and Eq. (17), the result will become as follows:

$$\frac{\partial^2}{\partial \mathrm{y}^2}\left[\frac{\partial^2\psi}{\partial \mathrm{y}^2} + \frac{n}{(1-n)}\,We\left(\frac{\partial^2\psi}{\partial \mathrm{y}^2}\right)^2\right] - \frac{\left(M^2\cos^2\dot{\beta} - \frac{1}{K} + \sigma^2\right)}{(1-n)}\frac{\partial^2\psi}{\partial \mathrm{y}^2} = 0 \quad (24)$$

4. Perturbation Solution

We can see that a closed form solution for all arbitrary parameters involved in eq.(16) is not achievable due to the complexity and high degree of nonlinearity of the equation. In order to determine the solution, perturbation approach is used. For perturbation solution, we can expand:

$\psi = \psi_0 + We\ \psi_1 + O(We^2)$.

$F = F_o + We\ F_1 + O(We^2)$.

$p = p_o + We\ p_1 + O(We^2)$, (25)

and substitute Eq.(25) into Eqs. (16)-(24) with boundary conditions Eqs.(18) and (19), by equating powers coefficients like of We, the result is given as follows :

4.1. Zero-order system:

$$\frac{\partial^4 \psi_0}{\partial y^4} - r^2 \frac{\partial^2 \psi_0}{\partial y^2} = 0. \quad (26)$$

Where

$$r^2 = \frac{\left(M^2 \cos^2 \dot{\beta} - \frac{1}{K} + \sigma^2\right)}{1-n}\ . \quad (27)$$

From Eq.(14),we get

$$\frac{\partial p_0}{\partial x} = \frac{\partial^3 \psi_0}{\partial y^3} - r^2\left(\frac{\partial \psi_0}{\partial y} + 1\right). \quad (28)$$

And from Eq.(15), we get

$$\frac{\partial p}{\partial y} = 0. \quad (29)$$

$$\psi_0 = {\psi_0}_{yy}{}^2. \quad (30)$$

$$\psi_0 = \frac{F_0}{2}, \frac{\partial \psi_0}{\partial y} = -1 \text{ at } y = h_1\ , \psi_0 = -\frac{F_0}{2}, \frac{\partial \psi_0}{\partial y} = -1 \text{ at } y = h_2\ . \quad (31)$$

4.2 First-order system

$$(1-n)\frac{\partial^4 \psi_1}{\partial y^4} - r^2 \frac{\partial^2 \psi_1}{\partial y^2} = -n \frac{\partial^2}{\partial y^2}\left[\left(\frac{\partial^2 \psi_0}{\partial y^2}\right)^2\right]. \quad (32)$$

$$\psi_1 = \frac{F_1}{2}, \frac{\partial \psi_1}{\partial y} = -1 \text{ at } y = h_1, \psi_1 = -\frac{F_1}{2}, \frac{\partial \psi_1}{\partial y} = -1 \text{ at } y = h_2\ . \quad (33)$$

$$\frac{\partial p_1}{\partial x} = (1-n)\frac{\partial^3 \psi_1}{\partial y^3} + n \frac{\partial^2}{\partial y^2}\left[\left(\frac{\partial^2 \psi_0}{\partial y^2}\right)^2\right] - r^2 \frac{\partial \psi_1}{\partial y}. \quad (34)$$

4.3 Solution to the Zeroth-order system

Eq. (26) is flowed and simplified, the results under conditions which are presented in Eq.(31) are obtained as follow:

$$\psi_0 = \frac{1}{e^{ry}}(e^{2ry}c1 + c2) + c3y + c4\ . \quad (35)$$

4.4 Solution to the First-order system

We have the following equations after the resultant equation system is solved with relevant boundary conditions and substituting 0^{th}-order solution into the 1^{st}-order system:

$$\psi_1 = e^{-2ry}\left(\frac{\frac{e^{4ry}(h1-h2)^2(-1+r)^2 r^4 n}{\xi}}{3m} + \frac{\frac{e^{2(h1+h2)r}(h1-h2)^2(1+r)^2 r^4 n}{\xi}}{3r^2} \frac{+3e^{3ry} * R1 + 3e^{ry} * R2)}{3r^2}\right) + R3 + y * R4\ . \quad (36)$$

Where

$$\xi = \begin{pmatrix} e^{\mathrm{h}2r}(-2 + \mathrm{h}1(-1+r^2)r - \mathrm{h}2(-1+r^2)r) + \\ e^{\mathrm{h}1r}(2 + \mathrm{h}1(-1+r^2)r - \mathrm{h}2(-1+r^2)\mathrm{r}) \end{pmatrix}^2 . \\ (-1+n)$$

The expression for stream function can be provided as follows:

$$\psi = \psi_0 + We\psi_1 . \quad (37)$$

Where {R1,R2,R3,R4, c1,c2,c3,c4,} are large quantities. It is mentioned in the appendix section.

The formula for the velocity is given as follows:

$$u = \psi_{0y} + We\psi_{1y} . \quad (38)$$

5. RESULTS AND DISCUSSION

There are two subsections within this section. In the first one, the flow properties are covered while in the other subsection, the trapping phenomena is demonstrated with the use of the MATHEMATICA software.

5.1 Flow characteristics

Based on Eq. (38). This section illustrates the impacts of different physical parameters on axial velocity profile including Weissenberg number We and Hartmann Number M, the porosity of porous media K, the inclination magnetic field angle $\dot{\beta}$, the hyperbolic tangent fluid power law index n, and impacts at each of σ, Q, Φ. Figures (2–9) show the velocity distributions graphically. Figure 2 shows how the Weissenberg number (We) effects axial velocity. It can be seen the velocity reduces when dimensionless parameter (We) is increased. Figure 3 shows how the Hartmann number (M) affects the axial velocity. It has been seen from this figure that the velocity increases in the channel centre, however, it drops at the walls as the dimensionless parameter (M) is increased. Figure 4 shows that if the velocity drops in the centre, it increases near walls with an increased value of $\dot{\beta}$. Figure 5 illustrates how the velocity increases as (Q) increases. The impact of the parameter σ on the velocity is presented in Figure 6. The velocity at walls has been shown to decrease as parameter σ is increased in Figure 6, and it has been noted that the velocity behaves in the opposite way near centre. It can be seen in Figure 7 that the velocity drops as the hyperbolic tangent fluid power law index n increases. Figure 8 demonstrates that as the porosity parameter K is increased, the velocity at the channel's centre increases. The impact of (Φ) on the axial velocity is finally depicted in Figure 9, where it can be initially noticed that the velocity falls but then it gradually increases as it approaches the channel's upper part. From these figures of velocity and from this work we can see that the magnetic field and the porosity are the most effective variables for regulating velocity and boluses in the peristaltic flow. We note that from the axial velocity graph, as the porosity parameter increased, the velocity of the fluid at the center of the channel increases, and if the increase of inclination magnetic field angle, then the walls of the channel draw the fluid in the wider section of channel so that the axial velocity is in the form of parabolic.

5.2 Trapping Phenomenon

The streamlines graph is plotted in this subsection to explain the trapping phenomenon. The trapping phenomenon represents the primary characteristic of peristaltic flow. Smooth streamlines are associated with the smooth flow. We can see that if waves are produced on the wavy walls, these streamlines become more curved which leads to the confinement of a bolus that moves with the flow. There are instances where the flow streamlines, divides, and produces boluses, closed-circulated trajectories that are carried by the peristaltic wave. The stream lines are presented in the non-uniform (lower panel $\Phi = \pi/3$) channels for various n, We, K, M, $\dot{\beta}$, σ, and Q values. The stream lines are displayed in Figures (10-16) for various parameter

values. Figures 10 and 15 show how We, n affect the stream lines. It has been observed that if any drop in We and n values, it results in the reduction in trapping bolus size, particularly towards the walls. It is clear from all figures that the stream lines closes to the channel almost exactly follow wall waves, primarily caused by the relative movement of walls. Figures 11 and 14 show that as the parameters M and σ are increased, the size of tapping bolus grows at non-uniform channel wall. Figures 12 and 13 show that new circulations (Bolus) are produced at left and right sides of channel, and that their size and quantity steadily rise with an increase in K but size of it's decreases with increase $\dot{\beta}$. In Figure 16, trapping bolus size is unchanged despite the increase of the value of Q, which results in a greater resistance and a slower of the fluid motion. Finally, We observe that by studying the effect of physical parameters on the streamlines, when the porosity increases, the size of the boluses increases but with increase of inclination magnetic field angle, the streamlines at the walls of the channel increased while the size of the boluses decreases, and this makes the movement of the fluid more streamlined within the channel.

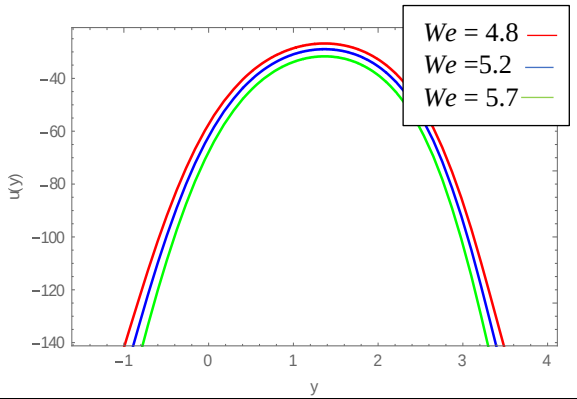

Figure 2: Effects of We on u(y)

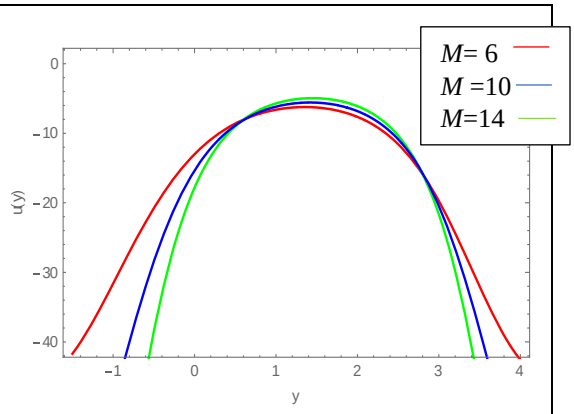

Figure 3: Effects of M on u(y)

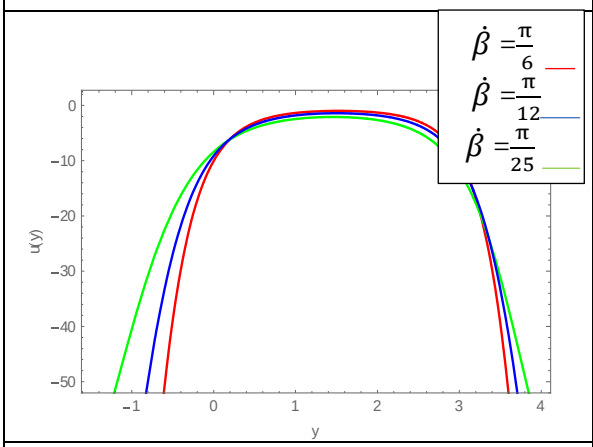

Figure 4: Effects of $\dot{\beta}$ on **u(y)**

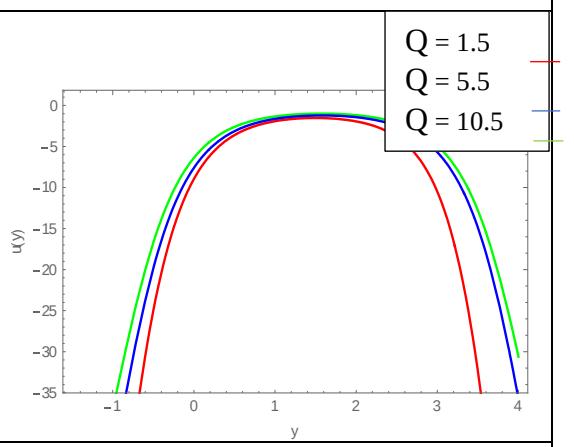

Figure 5: Effects of **Q** on **u(y)**

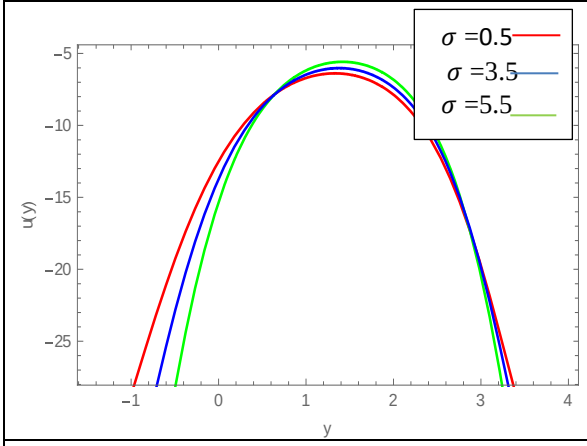

Figure 6: Effects of σ on **u(y)**

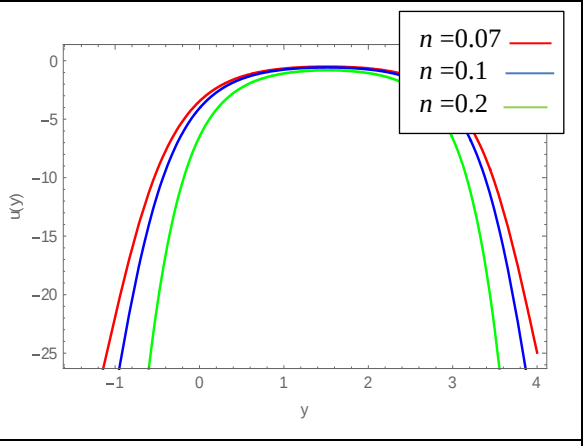

Figure 7: Effects of **n** on **u(y)**

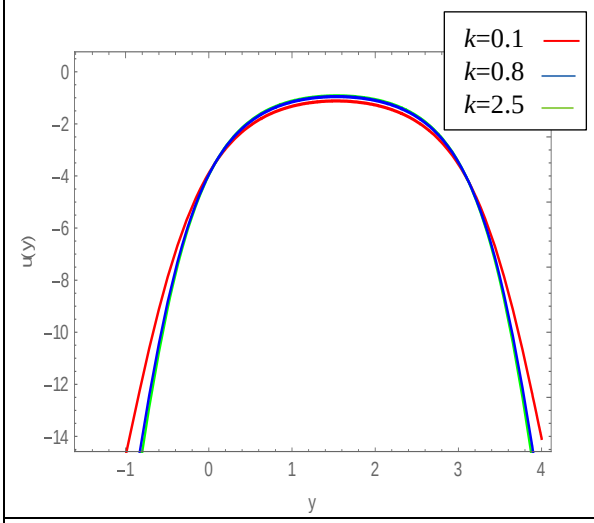

Figure8: Effects of **k** on **u(y)**

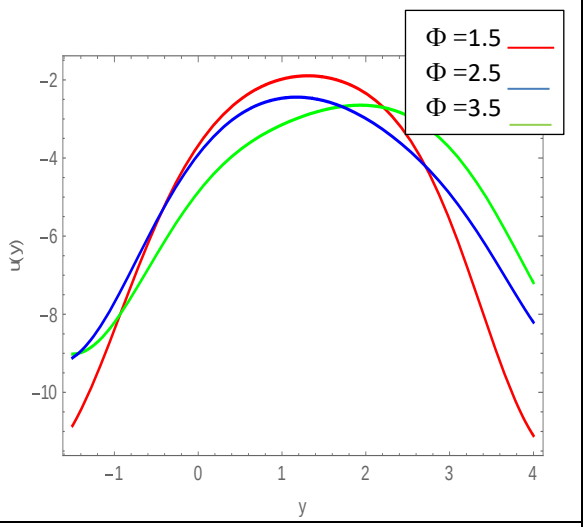

Figure9: Effects of **Φ** on **u(y)**

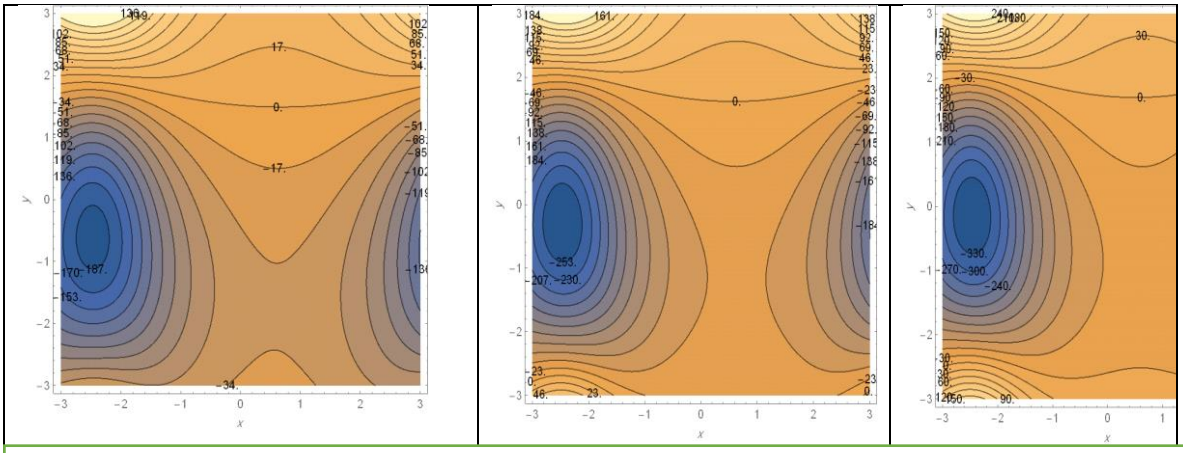

Figure 10: Stream-line for various ***We*** values: **(a)** ***We***=0.30,**(b)** ***We*** =0.50, & **(c)** ***We*** = 0.70, and $\Phi=\frac{\pi}{3}$,Q=1.50, d=1, a=0.50, b=0.50, σ=5, n=1, M=1,$\dot{\beta}=\frac{\pi}{6}$ and k=1.

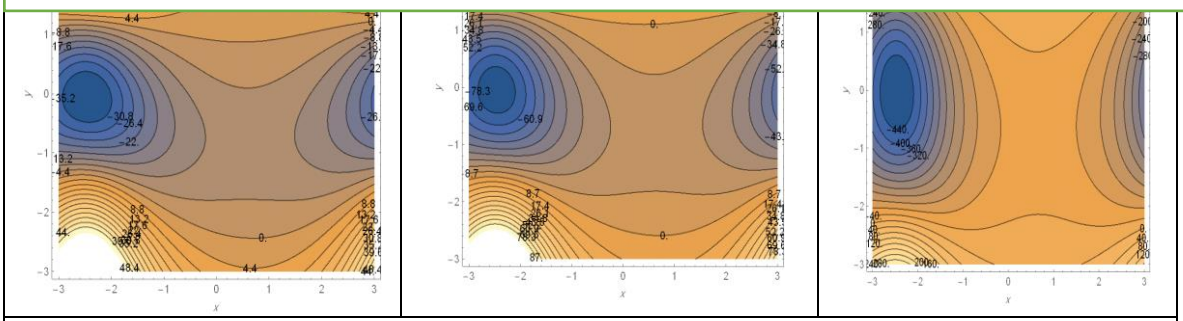

Figure11: Stream-line for various **M** values**: (a) M**=0.80,**(b) M**=0.90 and **(c) M** =1, and $\Phi=\frac{\pi}{3}$, Q=1.50, d=1, a=0.50, b=0.50, σ=5, n=1, We=1.5, $\dot{\boldsymbol{\beta}}=\frac{\pi}{6}$ and k=1.

(I) **(II)** **(III)**

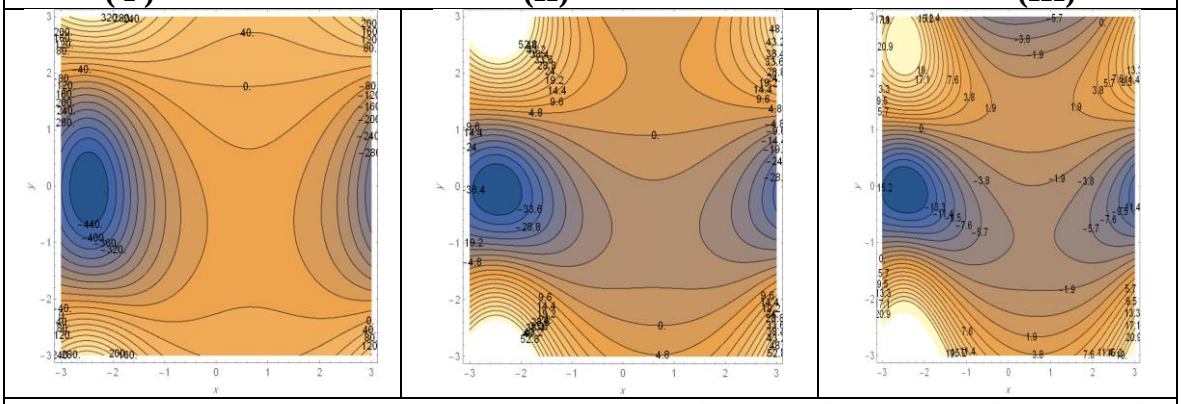

Figure12: Stream-line for various $\dot{\boldsymbol{\beta}}$ values: **(a)** $\dot{\boldsymbol{\beta}}=\frac{\pi}{6}$ **(b)** $\dot{\boldsymbol{\beta}}=\frac{\pi}{4}$ and **(c)** $\dot{\boldsymbol{\beta}}=\frac{\pi}{3}$, and $\Phi=\frac{\pi}{3}$, Q=1.50, d=1, a=0.50, b =0.50, σ=5, n=1, We=1.5, M=1 and k=1.

(I) **(II)** **(III)**

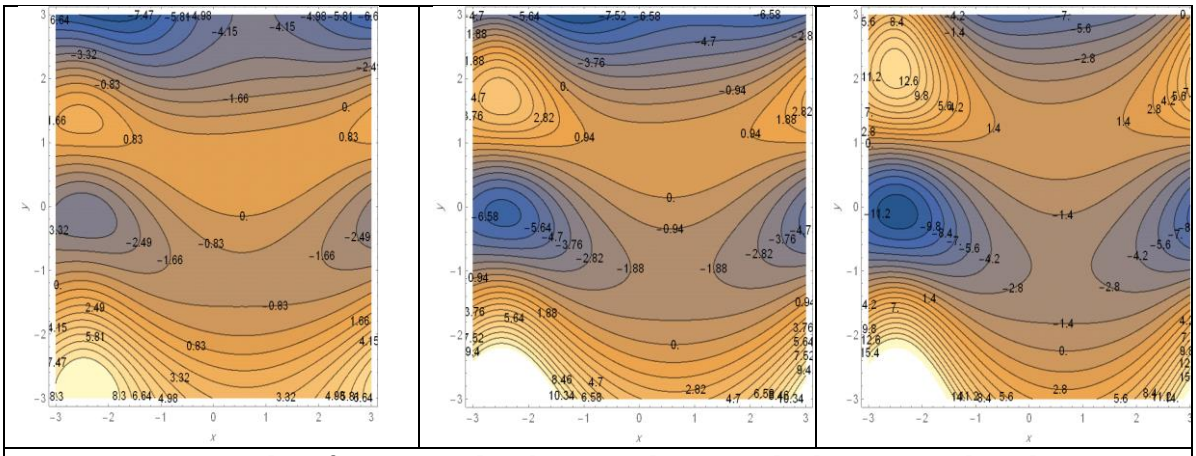

Figure 13. Stream-line for various ***k*** values***:*** **(a)** ***k*** =0.40, **(b)** ***k*** = 0.50 and **(c)** ***k*** = 0.60, & $\Phi=\frac{\pi}{3}$, Q=1.50, d=1, a=0.50, b=0.50, σ=5, n=1, M=1.50,$\dot{\beta}=\frac{\pi}{6}$ and We=1.

(I) **(II)** **(III)**

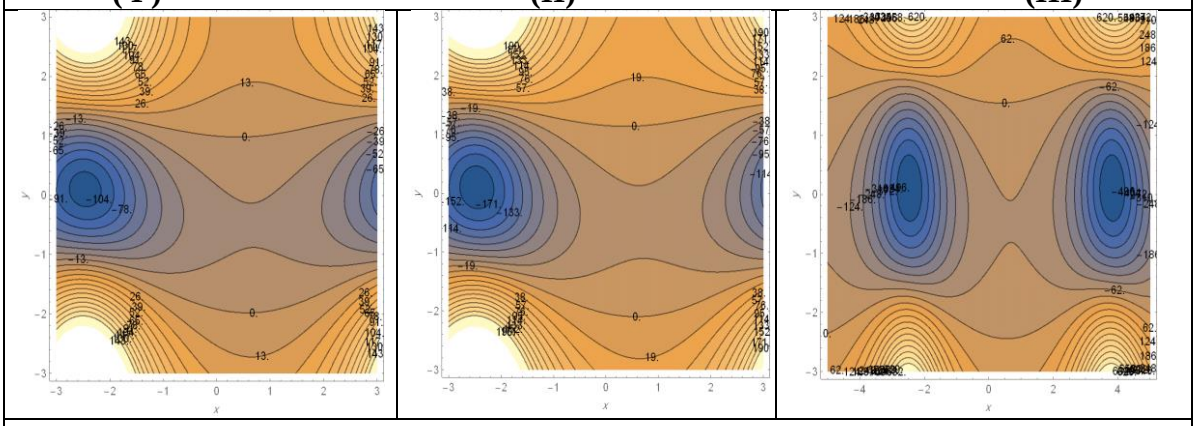

Figure 14: Stream-line for various $\boldsymbol{\sigma}$ values: **(a)** $\boldsymbol{\sigma}$ =0.20, **(b)** $\boldsymbol{\sigma}$ =0.30, and **(c)** $\boldsymbol{\sigma}$ = 0.40, and $\Phi=\frac{\pi}{3}$, Q=1.50, d=1, a=0.50, b=0.50, M=1, n=0.50, We=1.50, $\dot{\beta}=\frac{\pi}{6}$ and k=1.

(I) **(II)** **(III)**

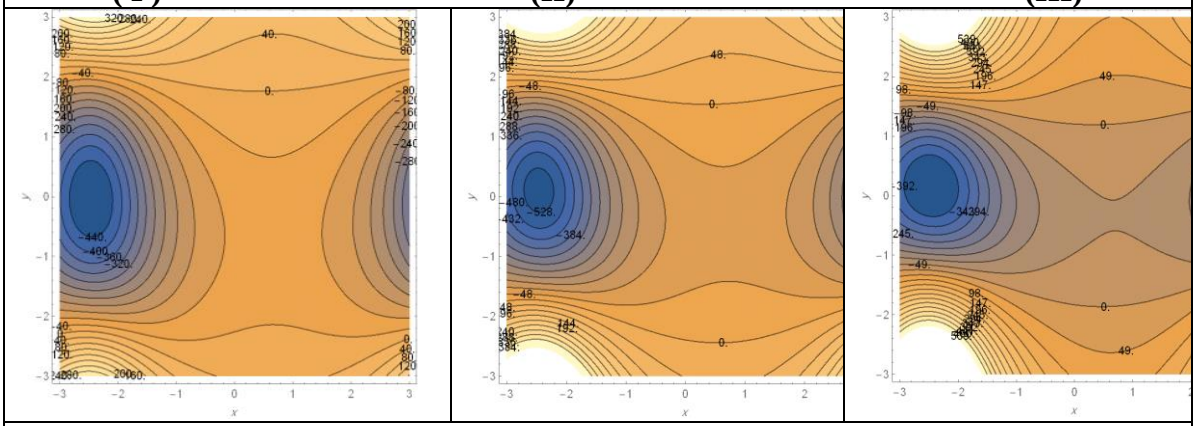

Figure15: Stream-line for various ***n*** values: (a) ***n*** = 0.30, (b) ***n*** = 0.50, and (c) ***n*** = 0.70, and $\Phi=\frac{\pi}{3}$, Q=1.50, d=1, a=0.50, b=0.50, σ=5, $\dot{\beta}=\frac{\pi}{6}$, We=1.50, M = 1 and k=1.

(I) **(II)** **(III)**

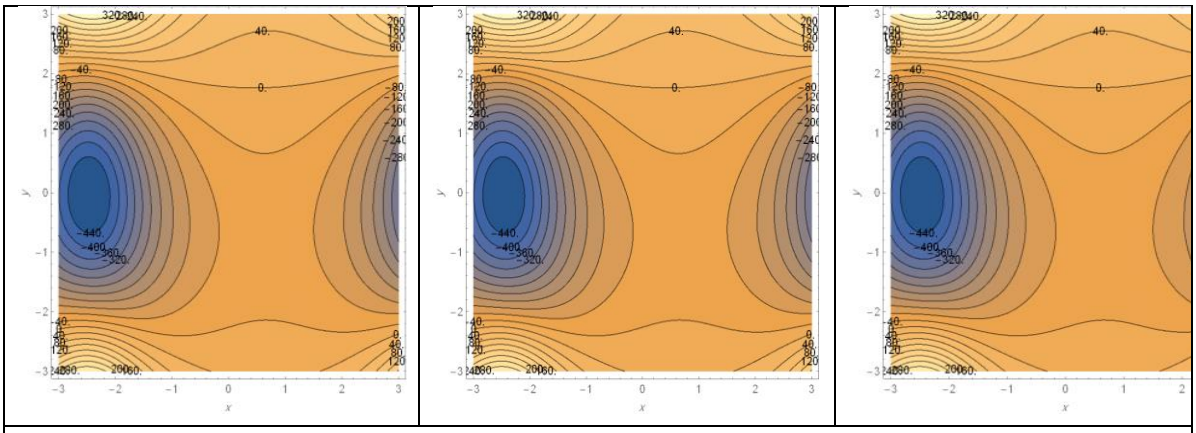

Figure 16: Stream-line for various **Q** values: **(a) Q** =0.50,**(b) Q** =1, and **(c) Q** = 1.50, Φ = $\frac{\pi}{3}$, *We*=1, d=1,
a=0.50, b=0.50, σ=5, *n*=1,M=1.50, $\dot{\beta}=\frac{\pi}{6}$ and k=1.
(I) **(II)** **(III)**

6. CONCLUSION

Under the action of the long wave-length approximations and low Reynolds number, the impact of inclined MHD peristaltic flow regarding non-Newtonian Hyperbolic Tangent fluid in 2D porous channel was examined in the current study. The axial velocity as well as streamline parameters of TANH fluid have been obtained using a regular perturbation approach. Depending on the present peristaltic transport mechanism through porous medium, the result flow patterns are examined and analyzed thoroughly for a variety of the values of various physical parameters in the flow region. The next findings are drawn from the current study:

- An increasing in ***We, n*** leads to decrease in the axial velocity, while, it increases with an increasing in value of **Q**.
- The velocity profile has been increased at center of channel with the increase in ***M, σ***, **K** while it reduces at the center with the increase in $\dot{\boldsymbol{\beta}}$.
- An increasing in **Φ** results in an increasing in the velocity regarding peristaltic flow at channel's upper wall.
- The streamlines illustrate that size of tapping bolus is increased with an increase in ***We, n***, whereas it reduces with the increase in ***M, σ***.
- It is also noticed that through the increase in **K** number , the size of trapping bolus increases, while with an increase $\dot{\boldsymbol{\beta}}$ number but the size of trapping bolus decreases. Finally, with an increase in Q value, size the bolus has not changed.
- Due to the many uses of the hyperbolic shadow fluid in biology. Blood flow and blood pump mechanics are examples of MHD peristaltic of a non-Newtonian Hyperbolic tangent fluid.

We draw the conclusion from this work that the magnetic field and porosity are the most effective variables for regulating velocity and boluses in the peristaltic flow.

Appendix

c

$$= -\left(\left((\mathrm{F0}+\mathrm{h1}-\mathrm{h2})r^2\right)/\left(-2e^{\mathrm{h1r}}+2e^{\mathrm{h2r}}+e^{\mathrm{h1r}}\mathrm{h1r}+e^{\mathrm{h2r}}\mathrm{h1r}-e^{\mathrm{h1r}}\mathrm{h2r}-e^{\mathrm{h2r}}\mathrm{h2r}\right)\right)$$

c2

$$= (e^{\mathrm{h1r}+\mathrm{h2r}}(\mathrm{F0}+\mathrm{h1}-\mathrm{h2})r^2)/(-2e^{\mathrm{h1r}}+2e^{\mathrm{h2r}}+e^{\mathrm{h1r}}\mathrm{h1r}+e^{\mathrm{h2r}}\mathrm{h1r}-e^{\mathrm{h1r}}\mathrm{h2r}-e^{\mathrm{h2r}}\mathrm{h2r})$$

c3

$$= -(((\mathrm{h1}+\mathrm{h2})(2e^{\mathrm{h1r}}-2e^{\mathrm{h2r}}+e^{\mathrm{h1r}}\mathrm{F0r}+e^{\mathrm{h2}\sqrt{m}}\mathrm{F0r}))/(2(-2e^{\mathrm{h1r}}+2e^{\mathrm{h2r}}+e^{\mathrm{h1}\sqrt{m}}\mathrm{h1r}+e^{\mathrm{h2r}}\mathrm{h1r}-e^{\mathrm{h1r}}\mathrm{h2r}-e^{\mathrm{h2r}}\mathrm{h2r})))$$

c4

$$= (2e^{\mathrm{h1r}} - 2e^{\mathrm{h2r}} + e^{\mathrm{h1r}}\mathrm{F0r} + e^{\mathrm{h2r}}\mathrm{F0r})/(-2e^{\mathrm{h1r}} + 2e^{\mathrm{h2r}} + e^{\mathrm{h1r}}\mathrm{h1r} + e^{\mathrm{h2r}}\mathrm{h1r} - e^{\mathrm{h1r}}\mathrm{h2r} - e^{\mathrm{h2r}}\mathrm{h2}r)$$

R1

$$= -((-(-\frac{e^{-\mathrm{h1}r}}{r^2} + \frac{e^{-\mathrm{h2r}}}{r^2}$$

$$+ \frac{e^{-\mathrm{h1r}}(-\mathrm{h1} + \mathrm{h2})}{r})(-((4e^{-2\mathrm{h1r}+2(\mathrm{h1}+\mathrm{h2})\mathrm{r}}(\mathrm{F0} + \mathrm{h1} - \mathrm{h2})^2 r^{3/2} n)/(3(e^{\mathrm{h1}r}(-2 + \mathrm{h1r} - \mathrm{h2r})\,(e^{\mathrm{h1r}}(-2$$

$$+ \mathrm{h1r} - \mathrm{h2r}) + e^{\mathrm{h2r}}(2 + \mathrm{h1r} - \mathrm{h2r}))^2(-1 + n))) + (4e^{-2\mathrm{h2r}+2(\mathrm{h1}+\mathrm{h2})\mathrm{r}}(\mathrm{F0} + \mathrm{h1} - \mathrm{h2})^2 r^{3/2} n)/$$

$$(3(e^{\mathrm{h1r}}(-2 + \mathrm{h1r} - \mathrm{h2r}) + e^{\mathrm{h2r}}(2 + \mathrm{h1r} - \mathrm{h2r}))^2(-1 + n)) +$$

$$(4e^{2\mathrm{h1r}}(\mathrm{F0} + \mathrm{h1} - \mathrm{h2})^2 r^{3/2} n)/\left(3\left(e^{\mathrm{h1r}}(-2 + \mathrm{h1r} - \mathrm{h2r}) + e^{\mathrm{h2r}}(2 + \mathrm{h1r} - \mathrm{h2r})\right)^2(-1 + n)\right) -$$

$$4e^{2\mathrm{h2r}}(\mathrm{F0} + \mathrm{h1} - \mathrm{h2})^2 r^{3/2} n)/(3(e^{\mathrm{h1r}}(-2 + \mathrm{h1r} - \mathrm{h2r}) + e^{\mathrm{h2r}}(2 + \mathrm{h1r} - \mathrm{h2r}))^2(-1 + n)))$$

$$+$$

$$(\frac{e^{-\mathrm{h1r}}}{\mathrm{r}} - \frac{e^{-\mathrm{h2r}}}{\mathrm{r}})(\mathrm{F1}$$

$$+ \left(2e^{-2\mathrm{h1r}+2(\mathrm{h1}+\mathrm{h2})\mathrm{r}}(\mathrm{F0} + \mathrm{h1} - \mathrm{h2})^2 rn\right)/(3(e^{\mathrm{h1r}}(-2 + \mathrm{h1r} - \mathrm{h2r}) + \ldots.$$

R2 $= (e^{-\mathrm{h1r}-\mathrm{h2r}} r^2(-12e^{4\mathrm{h1}r+2\mathrm{h2r}}\mathrm{F1} + 24e^{3\mathrm{h1r}+3\mathrm{h2r}}\mathrm{F1} - 12e^{2\mathrm{h1r}+4\mathrm{h2r}}\mathrm{F1}$

$$- 12e^{4\mathrm{h1r}+2\mathrm{h2r}}\mathrm{h1} +$$

$$24e^{3\mathrm{h1}r+3\mathrm{h2r}}\mathrm{h1} - 12e^{2\mathrm{h1r}+4\mathrm{h2r}}\mathrm{h1} + 12e^{4\mathrm{h1r}+2\mathrm{h2r}}\mathrm{h2} - 24e^{3\mathrm{h1r}+3\mathrm{h2r}}\mathrm{h2} + 12e^{2\mathrm{h1r}+4\mathrm{h2r}}\mathrm{h2}$$

$$+ 12e^{4\mathrm{h1r}+2\mathrm{h2r}}\mathrm{F1h1r} -$$

$$12e^{2\mathrm{h1}r+4\mathrm{h2r}}\mathrm{F1h1r} + 12e^{4\mathrm{h1r}+2\mathrm{h2r}}\mathrm{h1}^2\mathrm{r} - 12e^{2\mathrm{h1r}+4\mathrm{h2r}}\mathrm{h1}^2\mathrm{r} - 12e^{4\mathrm{h1r}+2\mathrm{h2r}}\mathrm{F1h2r}$$

$$+ 12e^{2\mathrm{h1r}+4\mathrm{h2r}}\mathrm{F1h2r} -$$

$$24e^{4\mathrm{h1}r+2\mathrm{h2r}}\mathrm{h1h2r} + 24e^{2\mathrm{h1r}+4\mathrm{h2r}}\mathrm{h1h2r} + 12e^{4\mathrm{h1r}+2\mathrm{h2r}}\mathrm{h2}^2\mathrm{r} - 12e^{2\mathrm{h1r}+4\mathrm{h2r}}\mathrm{h2}^2\mathrm{r}$$

$$- 3e^{4\mathrm{h1r}+2\mathrm{h2r}}\mathrm{F1h1}^2 r^2 - 6e^{3\mathrm{h1}r+3\mathrm{h2r}}\mathrm{F1h1}^2 r^2 - 3e^{2\mathrm{h1}r+4\mathrm{h2r}}\mathrm{F1h1}^2 r^2$$

$$- 3e^{4\mathrm{h1r}+2\mathrm{h2r}}\mathrm{h1}^3 r^2 - 6e^{3\mathrm{h1}r+3\mathrm{h2r}}\mathrm{h1}^3 r^2 - 3e^{2\mathrm{h1}r+4\mathrm{h2r}}\mathrm{h1}^3 r^2$$

$$+ 6e^{4\mathrm{h1}r+2\mathrm{h2r}}\mathrm{F1h1h2}r^2 + 12e^{3\mathrm{h1}r+3\mathrm{h2r}}\mathrm{F1h1h2}r^2 +$$

$$+6e^{2\mathrm{h1}r+4\mathrm{h2r}}\mathrm{F1h1h2}r^2 + 9e^{4\mathrm{h1}r+2\mathrm{h2r}}\mathrm{h1}^2\mathrm{h2}r^2 + 18e^{3\mathrm{h1}r+3\mathrm{h2r}}\mathrm{h1}^2\mathrm{h2}r^2$$

$$+ 9e^{2\mathrm{h1r}+4\mathrm{h2r}}\mathrm{h1}^2\mathrm{h2}r^2 - 3e^{4\mathrm{h1}r+2\mathrm{h2r}}\mathrm{F1h2}^2 r^2$$

$$6e^{3\mathrm{h1}r+3\mathrm{h2}r}\mathrm{F1h2}^2 r^2 - 3e^{2\mathrm{h1}r+4\mathrm{h2}r}\mathrm{F1h2}^2 r^2 - 9e^{4\mathrm{h1}r+2\mathrm{h2}r}\mathrm{h1h2}^2 r^2 -$$

$$18e^{3\mathrm{h1}r+3\mathrm{h2}r}\mathrm{h1h2}^2 r^2 - 9e^{2\mathrm{h1}r+4\mathrm{h2}r}\mathrm{h1h2}^2 r^2 + 3e^{4\mathrm{h1}r+2\mathrm{h2}r}\mathrm{h2}^3 r^2 + 6e^{3\mathrm{h1r}+3\mathrm{h2r}}\mathrm{h2}^3 r^2 +$$

$$3e^{2\mathrm{h1}r+4\mathrm{h2r}}\mathrm{h2}^3 r^2 +$$

$$12e^{4\mathrm{h1}r+2\mathrm{h2r}}\mathrm{F1}n - 24e^{3\mathrm{h1r}+3\mathrm{h2r}}\mathrm{F1}n + 12e^{2\mathrm{h1r}+4\mathrm{h2r}}\mathrm{F1}n + 12e^{4\mathrm{h1r}+2\mathrm{h2r}}\mathrm{h1}n$$

$$- 24e^{3\mathrm{h1r}+3\mathrm{h2r}}\mathrm{h1}n + \cdots$$

R3 $= -((e^{-2\mathrm{h1}r-2\mathrm{h2r}}(-24e^{5\mathrm{h1r}+2\mathrm{h2r}}\mathrm{h1} + 72e^{4\mathrm{h1r}+3\mathrm{h2r}}\mathrm{h1} - 72e^{3\mathrm{h1r}+4\mathrm{h2r}}\mathrm{h1}$

$$+ 24e^{2\mathrm{h1r}+5\mathrm{h2r}}\mathrm{h1}$$

$$-24e^{5\mathrm{h1}r+2\mathrm{h2r}}\mathrm{h2} + 72e^{4\mathrm{h1}r+3\mathrm{h2r}}\mathrm{h2} - 72e^{3\mathrm{h1r}+4\mathrm{h2r}}\mathrm{h2} + 24e^{2\mathrm{h1r}+5\mathrm{h2r}}\mathrm{h2}$$

$$- 12e^{5\mathrm{h1r}+2\mathrm{h2r}}\mathrm{F1h1r} + 12e^{4\mathrm{h1r}+3\mathrm{h2r}}\mathrm{F1h1r}$$

$$+12e^{3\mathrm{h1}r+4\mathrm{h2r}}\mathrm{F1h1r} - 12e^{2\mathrm{h1r}+5\mathrm{h2r}}\mathrm{F1h1r} + 24e^{5\mathrm{h1r}+2\mathrm{h2r}}\mathrm{h1}^2\mathrm{r} - 24e^{4\mathrm{h1r}+3\mathrm{h2r}}\mathrm{h1}^2\mathrm{r}$$

$$- 24e^{3\mathrm{h1r}+4\mathrm{h2r}}\mathrm{h1}^2\mathrm{r} + 24e^{2\mathrm{h1r}+5\mathrm{h2r}}\mathrm{h1}^2\mathrm{r} - 12e^{5\mathrm{h1r}+2\mathrm{h2r}}\mathrm{F1h2r}$$

$$+ 12e^{4\mathrm{h1r}+3\mathrm{h2r}}\mathrm{F1h2r} + 12e^{3\mathrm{h1r}+4\mathrm{h2r}}\mathrm{F1h2r} - 12e^{2\mathrm{h1r}+5\mathrm{h2r}}\mathrm{F1h2r}$$

$$- 24e^{5\mathrm{h1r}+2\mathrm{h2r}}\mathrm{h2}^2\mathrm{r} + 24e^{4\mathrm{h1r}+3\mathrm{h2r}}\mathrm{h2}^2\mathrm{r} + 24e^{3\mathrm{h1r}+4\mathrm{h2r}}\mathrm{h2}^2 r$$

$$- 24e^{2\mathrm{h1r}+5\mathrm{h2r}}\mathrm{h2}^2\mathrm{r} + 12e^{5\mathrm{h1r}+2\mathrm{h2r}}\mathrm{F1h1}^2\mathrm{r}^2 + 12e^{4\mathrm{h1r}+3\mathrm{h2r}}\mathrm{F1h1}^2\mathrm{r}^2$$

$$- 12e^{3\mathrm{h1r}+4\mathrm{h2r}}\mathrm{F1h1}^2\mathrm{r}^2 - 12e^{2\mathrm{h1}r+5\mathrm{h2r}}\mathrm{F1h1}^2\mathrm{r}^2$$

$$-6e^{5\mathrm{h1}r+2\mathrm{h2r}}\mathrm{h1}^3\mathrm{r}^2 - 6e^{4\mathrm{h1}r+3\mathrm{h2r}}\mathrm{h1}^3\mathrm{r}^2 + 6e^{3\mathrm{h1}r+4\mathrm{h2r}}\mathrm{h1}^3\mathrm{r}^2 + 6e^{2\mathrm{h1}r+5\mathrm{h2r}}\mathrm{h1}^3\mathrm{r}^2$$

$$+ 6e^{5\mathrm{h1r}+2\mathrm{h2r}}\mathrm{h1}^2\mathrm{h2}r^2 + 6e^{4\mathrm{h1}r+3\mathrm{h2r}}\mathrm{h1}^2\mathrm{h2}r^2 - 6e^{3\mathrm{h1}r+4\mathrm{h2r}}\mathrm{h1}^2\mathrm{h2}\mathrm{r}^2$$

$$-6e^{2\mathrm{h1}r+5\mathrm{h2r}}\mathrm{h1}^2\mathrm{h2}\mathrm{r}^2 - 12e^{5\mathrm{h1}r+2\mathrm{h2r}}\mathrm{F1h2}^2\mathrm{r}^2 - 12e^{4\mathrm{h1}r+3\mathrm{h2r}}\mathrm{F1h2}^2\mathrm{r}^2$$

$$+ 12e^{3\mathrm{h1r}+4\mathrm{h2r}}\mathrm{F1h2}^2\mathrm{r}^2 + 12e^{2\mathrm{h1}r+5\mathrm{h2r}}\mathrm{F1h2}^2\mathrm{r}^2 +$$

$$6e^{5h1r+2h2r}h1h2^2r^2+6e^{4h1r+3h2r}h1h2^2r^2-6e^{3h1r+4h2r}h1h2^2r^2-6e^{2h1r+5h2r}h1h2^2r^2$$
$$-6e^{5h1r+2h2r}h2^3r^2-6e^{4h1r+3h2r}h2^3r^2+6e^{3h1r+4h2r}h2^3r^2$$
$$+6e^{2h1r+5h2r}h2^3r^2-3e^{5h1r+2h2r}F1h1^3r^3-9e^{4h1r+3h2r}F1h1^3r^3-9e^{3h1r+4h2r}F1h1^3r^3$$
$$-3e^{2h1r+5h2r}F1h1^3r^3+$$
$$3e^{5h1r+2h2r}F1h1^2h2r^3+9e^{4h1r+3h2r}F1h1^2h2r^3+9e^{3h1r+4h2r}F1h1^2h2r^3$$
$$+3e^{2h1r+5h2r}F1h1^2h2r^3+3e^{5h1r+2h2r}F1h1h2^2r^3$$
$$+9e^{4h1r+3h2r}F1h1h2^2r^3+9e^{3h1r+4h2r}F1h1h2^2r^3+3e^{2h1r+5h2r}F1h1h2^2r^3$$
$$-3e^{5h1r+2h2r}F1h2^3r^3-9e^{4h1r+3h2r}F1h2^3r^3$$
$$-9e^{3h1r+4h2r}F1h2^3r^3-3e^{2h1r+5h2r}F1h2^3r^3+24e^{5hr+2h2r}h1n-72e^{4h1r+3h2r}h1n$$
$$+72e^{3h1r+4h2r}h1n-24e^{2h1r+5h2r}h1n+24e^{5hr+2h2r}h2n$$
$$-72e^{4h1r+3h2r}h2n+72e^{3h1r+4h2r}h2n-24e^{2h1r+5h2r}h2n$$
$$+12e^{5h1r+2h2r}F1h1rn-12e^{4h1r+3h2r}F1h1rn-\cdots$$

$$\mathbf{R4}=-((e^{-2h1r-2h2r}(24e^{5h1r+2h2r}-72e^{4h1r+3h2r}+72e^{3h1r+4h2r}-24e^{2h1r+5h2r}$$
$$+12e^{5h1r+2h2r}F1r$$
$$-12e^{4h1r+3h2r}F1r-12e^{3h1r+4h2r}F1r+12e^{2h1r+5h2r}F1r-24e^{5h1r+2h2r}h1r$$
$$+24e^{4h1r+3h2r}h1r+24e^{3h1r+4h2r}h1r$$
$$-24e^{2h1r+5h2r}h1r+24e^{5h1r+2h2r}h2r-24e^{4h1r+3h2r}h2r-24e^{3h1r+4h2r}h2r$$
$$+24e^{2h1r+5h2r}h2r-12e^{5h1r+2h2r}F1h1r^2-12e^{4h1r+3h2r}F1h1r^2$$
$$+12e^{3h1r+4h2r}F1h1r^2+12e^{2h1r+5h2r}F1h1r^2+6e^{5h1r+2h2r}h1^2r^2$$
$$+6e^{4h1r+3h2r}h1^2r^2-6e^{3h1r+4h2r}h1^2r^2-6e^{2h1r+5h2r}h1^2r^2$$
$$+12e^{5h1r+2h2r}F1h2r^2+12e^{4h1r+3h2r}F1h2r^2-12e^{3h1r+4h2r}F1h2r^2$$
$$-12e^{2h1r+5h2r}F1h2r^2-12e^{5h1r+2h2r}h1h2r^2-12e^{4h1r+3h2r}h1h2r^2$$
$$+12e^{3h1r+4h2r}h1h2r^2+12e^{2h1r+5h2r}h1h2r^2+$$
$$6e^{5h1r+2h2r}h2^2r^2+6e^{4h1r+3h2r}h2^2r^2-6e^{3h1r+4h2r}h2^2r^2-6e^{2h1r+5h2r}h2^2r^2+$$
$$+3e^{5h1r+2h2r}F1h1^2r^3+9e^{4h1r+3h2r}F1h1^2r^3+9e^{3h1r+4h2r}F1h1^2r^3+$$
$$3e^{2h1r+5h2r}F1h1^2r^3-6e^{5h1r+2h2r}F1h1h2r^3$$
$$-18e^{4h1r+3h2r}F1h1h2r^3-18e^{3h1r+4h2r}F1h1h2r^3-6e^{2h1r+5h2r}F1h1h2r^3$$
$$+3e^{5h1r+2h2r}F1h2^2r^3+9e^{4h1r+3h2r}F1h2^2r^3$$
$$+9e^{3h1r+4h2r}F1h2^2r^3+3e^{2h1r+5h2r}F1h2^2r^3-24e^{5h1r+2h2r}n+72e^{4h1r+3h2r}n$$
$$-72e^{3h1r+4h2r}n+24e^{2h1r+5h2r}n-12e^{5h1r+2h2r}F1rn+$$
$$12e^{4h1r+3h2r}F1rn+12e^{3h1r+4h2r}F1rn-12e^{2h1r+5h2r}F1rn+24e^{5h1r+2h2r}h1rn$$
$$-24e^{4h1r+3h2r}h1rn-24e^{3h1r+4h2r}h1rn+24e^{2h1r+5h2r}h1rn$$
$$-24e^{5h1r+2h2r}h2rn+24e^{4h1r+3h2r}h2rn+24e^{3h1r+4h2r}h2rn$$
$$-24e^{2h1r+5h2r}h2rn+12e^{5h1r+2h2r}F1h1r^2n$$
$$+12e^{4h1r+3h2r}F1h1r^2n-12e^{3h1r+4h2r}F1h1r^2n-12e^{2h1r+5h2r}F1h1r^2n-$$
$$6e^{5h1r+2h2r}h1^2r^2n-6e^{4h1r+3h2r}h1^2r^2n+6e^{3h1r+4h2r}h1^2r^2n\quad+6e^{2h1r+5h2r}h1^2r^2n-$$
$$12e^{5h1r+2h2r}F1h2r^2n-12e^{4h1r+3h2r}F1h2r^2n+12e^{3h1r+4h2r}F1h2r^2n+$$
$$12e^{2h1r+5h2r}F1h2r^2n+12e^{5h1r+2h2r}h1h2r^2n+$$
$$12e^{4h1r+3h2r}h1h2r^2n-12e^{3h1r+4h2r}h1h2r^2n-12e^{2h1r+5h2r}h1h2r^2n-$$
$$6e^{5h1r+2h2r}h2^2r^2n-6e^{4h1r+3h2r}h2^2r^2n+6e^{3h1r+4h2r}h2^2r^2n+\ldots$$

Acknowledgment

We thank the reviewers for the constructive and helpful comments. Important aspects in the paper are highlighted, which lead to an important and clear improvement to this paper.

References

[1] T. W. Latham, "Fluid motions in a peristaltic pump," 1966. [Online]. Available: https://dspace.mit.edu/handle/1721.1/17282.

[2] A. H. Shapiro, M. Y. Jaffrin, and S. L. Weinberg, "Peristaltic pumping with long wavelengths at low Reynolds number," *J. Fluid Mech*, vol. 37, no. 4, pp. 799–825, 2016, doi: 10.1017/S0022112069000899.

[3] Y. C .Fung and C.S. Yih, "Peristaltic Transport, " *ASME J. Fluid Mech*, vol. 36, no. 2, pp. 669–675, 1968, doi: 10.1115/1.3564676.

[4] I. I. Pop and D. B. Ingham, *Convective heat transfer :* " *mathematical and computational modelling of viscous fluids and porous media*,". Pergamon, 2001. [Online]. Available: http://www.sciencedirect.com:5070/book/9780080438788/convective-heat-transfer.

[5] S. Nadeem and S. Akram, "Peristaltic Transport of a Hyperbolic Tangent Fluid Model in an Asymmetric Channel, " 2009. [Online]. Available: http://znaturforsch.com.

[6] S. Nadeem and E. N. Maraj, " The Mathematical Analysis for Peristaltic Flow of Hyperbolic Tangent Fluid in a Curved Channel," 2013. [Online]. Available: http://ctp.itp.ac.cn.

[7] N. B. Naduvinamani, A. S. Guttedar, U. Shankar, and H. Basha, "Exploration of the dynamics of hyperbolic tangent fluid through a tapered asymmetric porous channel," *NLE*, vol. 11, no. 1, pp. 298–315, 2022, doi: 10.1515/NLENG-2022-0033.

[8] T. Hayat, M. Rafiq, and B. Ahmad, "Soret and Dufour Effects on MHD Peristaltic Flow of Jeffrey Fluid in a Rotating System with Porous Medium," *PLoS One*, vol. 11, no. 1, p. e0145525, 2016, doi: 10.1371/JOURNAL.PONE.0145525.

[9] S. Nadeem and S. Akram, "Magnetohydrodynamic peristaltic flow of a hyperbolic tangent fluid in a vertical asymmetric channel with heat transfer," *Acta Mechanica Sinica/Lixue Xuebao*, vol. 27, no. 2, pp. 237–250, 2011, doi: 10.1007/S10409-011-0423-2/METRICS.

[10] R. Saravana *et al.*, "MHD peristaltic flow of a hyperbolic tangent fluid in a non-uniform channel with heat and mass transfer," In *IOP Conference Series: Materials Science and Engineering* vol. 263, No. 6, p. 062006. IOP Publishing, 2017, doi: 10.1088/1757-899X/263/6/062006.

[11] M. Kothandapani and S. Srinivas, "On the influence of wall properties in the MHD peristaltic transport with heat transfer and porous medium," *Phys Lett A*, vol. 372, no. 25, pp. 4586–4591, 2008, doi: 10.1016/J.PHYSLETA.2008.04.050 .

[12] K. Das, "Influence of slip and heat transfer on MHD peristaltic flow of a Jeffrey fluid in an inclined asymmetric porous channel," 2012. [Online]. Available: https://www. researchgate. net/publication/266994452.

[13] K. Ramesh and M. Devakar, "Magnetohydrodynamic peristaltic transport of couple stress fluid through porous medium in an inclined asymmetric channel with heat transfer," *J Magn Magn Mater*, vol. 394, pp. 335–348, Nov. 2015, doi: 10.1016/J.JMMM.2015.06.052.

[14] T. Hayat, A. Saleem, A. Tanveer, and F. Alsaadi, "Numerical study for MHD peristaltic flow of Williamson nanofluid in an endoscope with partial slip and wall properties," *Int J Heat Mass Transf*, vol. 114, pp. 1181–1187, 2017, doi: 10.1016/J.IJHEATMASSTRANSFER.2017.06.066.

[15] M. Veera Krishna, K. Bharathi, and A. J. Chamkha, "Hall effects on Mhd peristaltic flow of Jeffrey fluid through porous medium in a vertical stratum," *Interfacial Phenom Heat Transf*, vol. 6, no. 3, pp. 253–268, 2018, doi: 10.1615/INTERFACPHENOMHEATTRANSFER.2019030215.

[16] H. Vaidya, C. Rajashekhar, B. B. Divya, G. Manjunatha, K. V. Prasad, and I. L. Animasaun, "Influence of transport properties on the peristaltic MHD Jeffrey fluid flow through a porous asymmetric tapered channel," *Results Phys*, vol. 18, p. 103295, 2020, doi: 10.1016/J.RINP.2020.103295.

[17] R. S. Kareem and A. M. Abdulhadi, "Impacts of heat and mass transfer on magneto hydrodynamic peristaltic flow having temperature-dependent properties in an inclined channel through porous media," *Iraqi Journal of Science*, vol. 61, no. 4, pp. 854–869, 2020, doi: 10.24996/ijs.2020.61.4.19.

[18] S. S. Hasen and A. M. Abdulhadi, "MHD effect on peristaltic transport for rabinowitsch fluid through a porous medium in cilia channel," *Iraqi Journal of Science*, vol. 61, no. 6, pp. 1461–1472, 2020, doi: 10.24996/ijs.2020.61.6.26.

[19] N. T. M. El-Dabe, M. Y. Abou-Zeid, M. A. A. Mohamed, and M. M. Abd-Elmoneim, "MHD peristaltic flow of non-Newtonian power-law nanofluid through a non-Darcy porous medium

inside a non-uniform inclined channel," *Archive of Applied Mechanics*, vol. 91, no. 3, pp. 1067–1077, 2021, doi: 10.1007/S00419-020-01810-3.

[20] N. Sher Akbar, S. Akbar, and Noreen, "Influence of magnetic field on peristaltic flow of a Casson fluid in an asymmetric channel: Application in crude oil refinement," *JMMM*, vol. 378, pp. 463–468, 2015, doi: 10.1016/J.JMMM.2014.11.045.

[21] M. Rashid, K. Ansar, and S. Nadeem, "Effects of induced magnetic field for peristaltic flow of Williamson fluid in a curved channel," *Physica A: Statistical Mechanics and its Applications*, vol. 553, p. 123979, 2020, doi: 10.1016/J.PHYSA.2019.123979.

[22] G. Sucharitha, M. M. Rashidi, S. Sreenadh, and P. Lakshminarayana, "Effects of magnetic field and slip on convective peristaltic flow of a non-Newtonian fluid in an inclined nonuniform porous channel with flexible walls," *J Porous Media*, vol. 21, no. 10, pp. 895–910, 2018, doi: 10.1615/JPORMEDIA.2018020133.

[23] M. Kothandapani and J. Prakash, "The peristaltic transport of carreau nanofluids under effect of a magnetic field in a tapered asymmetric channel: Application of the cancer therapy," *J Mech Med Biol*, vol. 15, no. 3, 2015, doi: 10.1142/S021951941550030X.

[24] S. Akram, A. Razia, M. Y. Umair, T. Abdulrazzaq, and R. Z. Homod, "Double-diffusive convection on peristaltic flow of hyperbolic tangent nanofluid in non-uniform channel with induced magnetic field," *Math Methods Appl Sci*, vol. 46, no. 10, pp. 11550–11567, 2023, doi: 10.1002/MMA.8188.

[25] Yellamma *et al.*, "Triple diffusive Marangoni convection in a fluid-porous structure: Effects of a vertical magnetic field and temperature profiles," *Case Studies in Thermal Engineering*, vol. 43, p. 102765, Mar. 2023, doi: 10.1016/J.CSITE.2023.102765.

[26] V. K. Balaji, M. Narayanappa, R. Udhayakumar, G. AlNemer, S. Ramakrishna, and G. Y. Honnappa, "Effects of LTNE on Two-Component Convective Instability in a Composite System with Thermal Gradient and Heat Source," *Mathematics 2023, Vol. 11, Page 4282*, vol. 11, no. 20, p. 4282, doi: 10.3390/MATH11204282.

[27] N. Manjunatha and R. Sumithra, "Non-Darcian-Bènard Double Diffusive Magneto-Marangoni Convection in a Two Layer System with Constant Heat Source/Sink," *Iraqi Journal of Science*, vol. 62, no. 11, pp. 4039–4055, Nov. 2021, doi: 10.24996/ijs.2021.62.11.24.

[28] R. Sumithra and N. Manjunatha, "Effects of Heat Source/ Sink and non uniform temperature gradients on Darcian-Bènard -Magneto-Marangoni convection in composite layer horizontally enclosed by adiabatic boundaries," *Malaya Journal of Matematik*, vol. 8, no. 2, pp. 373–382, 2020, doi: 10.26637/mjm0802/0010.

[29] T. Hayat, S. Bibi, M. Rafiq, A. Alsaedi, and F. M. Abbasi, "Effect of an inclined magnetic field on peristaltic flow of Williamson fluid in an inclined channel with convective conditions," *J Magn Magn Mater*, vol. 401, pp. 733–745, 2016, doi: 10.1016/J.JMMM.2015.10.107.

[30] S. Akram and Q. Afzal, "Effects of thermal and concentration convection and induced magnetic field on peristaltic flow of Williamson nanofluid in inclined uniform channel," *Eur Phys J Plus*, vol. 135, no. 10, 2020, doi: 10.1140/EPJP/S13360-020-00869-9.

[31] B. B. Divya, G. Manjunatha, C. Rajashekhar, H. Vaidya, and K. V. Prasad, "Effects of Inclined Magnetic Field and Porous Medium on Peristaltic Flow of a Bingham Fluid with Heat Transfer," *Journal of Applied and Computational Mechanics*, vol. 7, no. 4, pp. 1892–1906, 2021, doi: 10.22055/JACM.2019.31060.1822.

[32] F. A. Adnan and A. M. A. Hadi, "Effect of an inclined magnetic field on peristaltic flow of Bingham plastic fluid in an inclined symmetric channel with slip conditions," *Iraqi Journal of Science*, vol. 60, no. 7, pp. 1551–1574, 2019, doi: 10.24996/ijs.2019.60.7.16.

[33] S. R. Ridha, "A Review Report of Present Trend in Peristaltic Activity of MHD NON-Newtonian and Newtonian Fluids," Journal of AL-Farabi for Engineering Sciences , vol. 1, no. 2, pp. 9–9, 2022, doi: 10.59746/JFES.V1I2.40.